Electronic Supplementary Material (ESI) for Physical Chemistry Chemical Physics.

Supporting Information for Molecular Dynamics Simulations of Alkaline Earth Metal Ions Binding to DNA Reveal Ion Size and Hydration Effects

Makenzie Provorse Long,[*,†] *Serra Alland,*[†] *Madison E. Martin,*[†] *and Christine M. Isborn*[‡]

[†]Department of Chemistry and Biochemistry, University of Central Arkansas, Conway, Arkansas 72035, USA

[‡]Chemistry and Chemical Biology, University of California Merced, Merced, California 95343, USA

Corresponding Author

* E-mail: mlong14@uca.edu

Computational Details

Molecular Simulations

Table S1 Lennard-Jones force field parameters of divalent metal ions.

Fig. S1 Average number of divalent metal ions bound to dsDNA.

Table S2 Average number of divalent metal ions bound to dsDNA with error.

Fig. S2 Radial distribution functions of ions and DNA phosphate backbone.

Analysis

Table S3 Occupancy of dsDNA by Sr^{2+} and Ba^{2+} computed with 20 and 100 frames.

Additional Simulations

Results and Discussion

Validation of Divalent Metal Ion Force Field

Table S4 Excess number of divalent ions associated with dsDNA.

Fig. S3 Occupancy of dsDNA by monovalent and divalent metal ions.

Table S5 Ion-phosphate distances.

DNA Binding Sites

Fig. S4 Classification of indirect contacts between divalent metal ions and the phosphate backbone of dsDNA.

Fig. S5 Classification of direct contacts or simultaneous direct and indirect contacts between divalent metal ions and the phosphate backbone of dsDNA.

Fig. S6 Radial distribution functions of divalent metal ions and electronegative atoms in the minor groove of dsDNA.

Fig. S7 Radial distribution functions of divalent metal ions and electronegative atoms in the major groove of dsDNA.

Fig. S8 Classification of indirect contacts between divalent metal ions and the major groove of dsDNA.

Quantitative Analysis of DNA-Ion Binding

Table S6 Occupancy values of DNA binding sites by divalent metal ions.

Sequence-Dependent Binding in Major Groove

Fig. S9 Occupancy of DNA base pairs at phosphate backbone and major groove.

Major Groove Binding at Guanine N7 and O6 Atoms

Fig. S10 Occupancy of N7 and O6 atoms of guanine by divalent metal ions classified by shortest distance.

Overall Comparison of Alkaline Earth Metal Ions

Fig. S11 Occupancy of dsDNA by Ca^{2+}, Sr^{2+}, and Ba^{2+} classified by the number of water molecules within their first solvation shells.

Fig. S12 Average number of binding events per ion.

Fig. S13 Distribution of DNA-ion residence times.

Computational Details

Molecular Simulations

The Lennard-Jones parameters[1] used to model divalent metal ions in this study are shown in Table S1.

Table S1 Lennard-Jones force field parameters of divalent metal ions.

ion	σ (nm)	ε (kJ/mol)
Ni^{2+}	2.236×10^{-1}	1.09755×10^{-2}
Co^{2+}	2.315×10^{-1}	2.02460×10^{-2}
Mg^{2+}	2.423×10^{-1}	4.26867×10^{-2}
Ca^{2+}	2.938×10^{-1}	4.43205×10^{-1}
Sr^{2+}	3.225×10^{-1}	9.26018×10^{-1}
Ba^{2+}	3.597×10^{-1}	1.70141

The convergence of each production simulation is evaluated by the total number of divalent metal ions bound to dsDNA, where a bound ion is defined as being within 5 Å (Ni^{2+}, Co^{2+}, and Mg^{2+}) or 6 Å (Ca^{2+}, Sr^{2+}, and Ba^{2+}) of any DNA atom. These radial distances include the first and second solvation shells of each ion, which corresponds to both direct and indirect binding. The average number of divalent ions bound to DNA computed for 50 ns intervals of each production simulation is shown in Fig. S1. The Ni^{2+} and Co^{2+} simulations are relatively converged for the entire 300 ns of their production simulations because the average number of

divalent ions bound to DNA fluctuates by less than 1 ion. The average number of Mg^{2+} ions bound to DNA decreases by approximately 1 ion near 300 ns, but increases by a similar value near 400 ns and, thus, is considered converged throughout its 500 ns production simulation. The Ca^{2+} simulation has a large increase in average number of divalent ions bound to DNA within the first 100 ns of the production simulation. To ensure that this is not an artifact of the initial placement of the divalent ions relative to the DNA duplex, a second Ca^{2+} simulation was performed using the same simulation setup, but different initial coordinates for the divalent and monovalent ions relative to the DNA duplex. This simulation is denoted as 'Ca new' in Fig. S1 and also has a large increase in the average number of divalent ions bound to DNA within the 100 ns of the simulation. Therefore, the large number of Ca^{2+} bound to DNA is not an artifact of the initial ion placement relative to the DNA duplex. The Ca^{2+}, Sr^{2+}, and Ba^{2+} simulations display larger fluctuations in the average number of bound divalent ions compared to the Ni^{2+}, Co^{2+}, and Mg^{2+} simulations that warrant quantitative analysis of production simulation convergence.

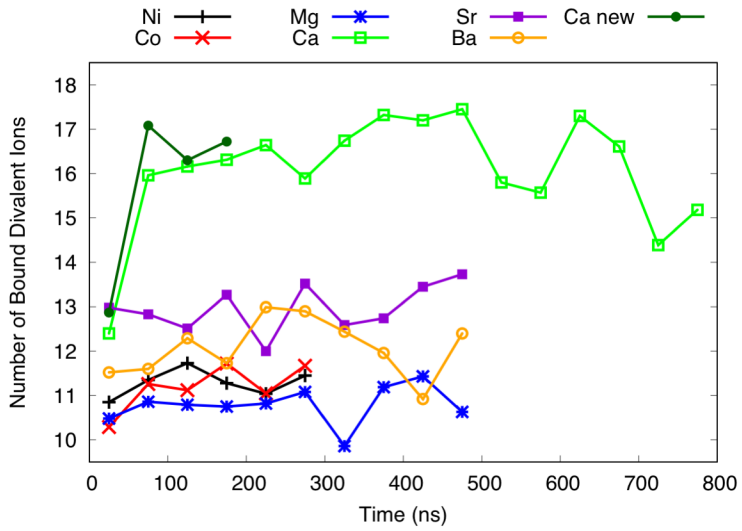

Fig. S1 Average number of divalent metal ions bound to dsDNA.

The average number of divalent metal ions bound to dsDNA computed for the total production simulation and the last 250 ns (Ni^{2+} and Co^{2+}), 450 ns (Mg^{2+}, Sr^{2+}, and Ba^{2+}) or 750 ns (Ca^{2+}) of the production simulation are shown in Table S2. Error is reported as the standard deviation of the data points shown in Fig. S1. By removing the first 50 ns of each production simulation, the maximum error decreases from about 2 ions to less than 1 ion. The absolute value of the largest difference between average values computed between 100 ns and 200 ns and the average value computed without the first 50 ns of each simulation is shown in parentheses in Table S2. This value is less than 0.5 ions for all simulations; therefore the 100 ns to 200 ns portion of each production simulation reproduces the average value of the converged production simulations and is used for additional analysis.

Table S2 Average number of divalent metal ions bound to dsDNA.[a]

simulation	total production simulation[b]	without first 50 ns[c]
Ni^{2+}	11.28 ± 0.31	11.37 ± 0.25 (0.36)
Co^{2+}	11.19 ± 0.52	11.36 ± 0.31 (0.36)
Mg^{2+}	10.79 ± 0.43	10.82 ± 0.44 (0.07)
Ca^{2+}	16.06 ± 1.29	16.30 ± 0.87 (0.14)
Sr^{2+}	12.96 ± 0.53	12.96 ± 0.57 (0.45)
Ba^{2+}	12.08 ± 0.65	12.14 ± 0.66 (0.41)
Ca^{2+} new coordinates[d]	15.74 ± 1.94	16.70 ± 0.39 (0.40)

a Number of bound ions is calculated using mindist GROMACS tool, where the maximum distance between a bound ion and any DNA atom is 5 Å (Ni^{2+}, Co^{2+}, and Mg^{2+}) or 6 Å (Ca^{2+}, Sr^{2+}, and Ba^{2+}). Error is reported as standard deviation of 50-ns average values.

b Total production simulation time: 300 ns (Ni^{2+} and Co^{2+}), 500 ns (Mg^{2+}, Sr^{2+}, and Ba^{2+}), 800 ns (Ca^{2+}), or 200 ns (Ca^{2+} new coordinates).

c Total production simulation time without the first 50 ns of each simulation. Error in parentheses is the largest absolute deviation from values computed between 100 ns and 200 ns and the average value computed without the first 50 ns of each simulation.

d Ca^{2+} simulation using different initial coordinates for the divalent and monovalent ions.

Previous work[2] identified unphysical ion pair formation in atomistic molecular dynamics simulations of Ca^{2+} ions bound to dsDNA. The radial distribution functions (RDFs) between the oxygen atoms of the DNA phosphate backbone and divalent metal ions (Mg^{2+} or Ca^{2+}), monovalent metal ions (Na^{+}), and anions (Cl^{-}) are shown in Fig. S2. The relative probability of finding a Cl^{-} ion within 10 Å of the DNA phosphate backbone is negligible. This probability

approaches 1.0 as the radial distance increases, indicating bulk ion behavior at large distances from dsDNA. In both simulations, the Na^+ ion RDFs have two peaks near DNA that represent direct and indirect binding between Na^+ and the oxygen atoms of the phosphate backbone. These peaks occur at similar distances reported by previous atomistic molecular dynamics simulations of Na^+ with dsDNA.[3]

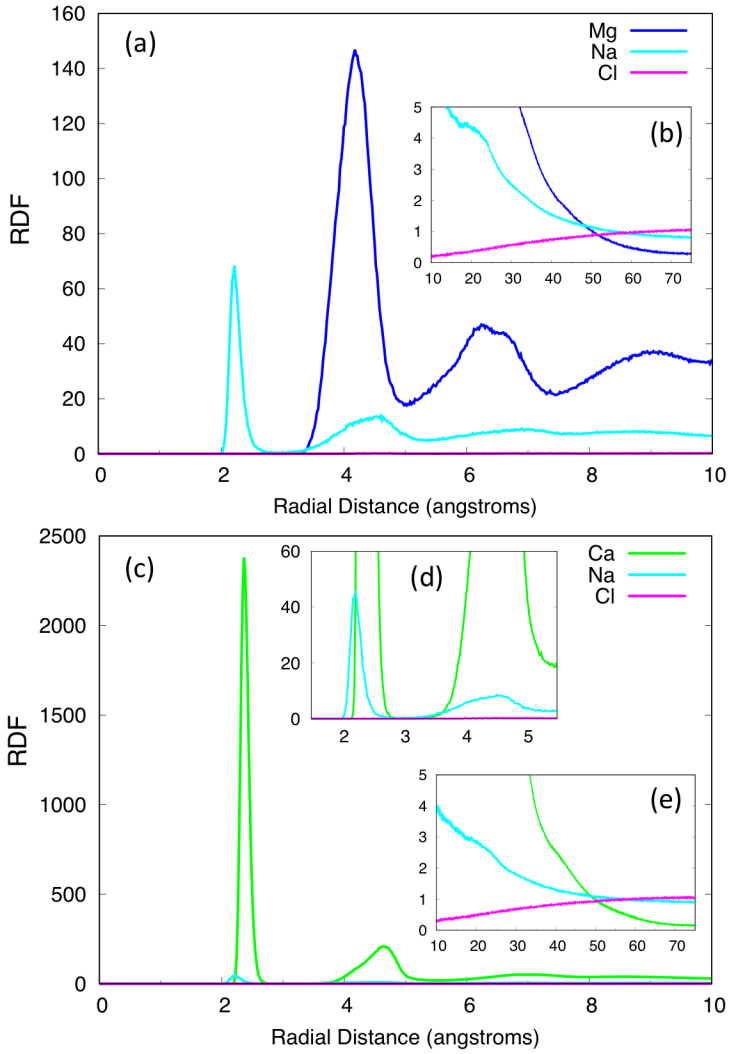

Fig. S2 The RDFs between the oxygen atoms of the DNA phosphate backbone and divalent metal ions (Mg^{2+} or Ca^{2+}), monovalent metal ions (Na^+), and anions (Cl^-). RDFs computed from a 500-ns simulation with Mg^{2+} are shown in panels (a) and (b). RDFs computed from the first 500 ns of an 800-ns simulation with Ca^{2+} are shown in panels (c), (d), and (e).

Analysis

Convergence of production simulations with respect to sampling was evaluated by comparing occupancy values of Sr^{2+} and Ba^{2+} computed between 100 ns and 200 ns of each production simulation using 20 frames saved every 5 ns versus 100 frames saved every 1 ns (Table S3). Similar trends in occupancy are observed between ions and among binding sites when 20 versus 100 frames are used. With increased sampling, the total occupancy increases by 0.0010 for Sr^{2+} and decreases by 0.0135 for Ba^{2+}. Occupancy of specific binding sites changes by no more than 0.0105. These changes in occupancy correspond to less than 1 ion changing binding sites throughout the sampling time, which is consistent with the level of convergence reported with respect to simulation time.

Table S3 Occupancy of dsDNA by Sr^{2+} and Ba^{2+} computed with 20 and 100 frames.

binding site	Sr^{2+}		Ba^{2+}	
	20 frames	100 frames	20 frames	100 frames
total occupancy	0.6075	0.6085	0.5825	0.5690
phosphate backbone	0.4550	0.4595	0.3825	0.3780
major groove	0.0950	0.0850	0.1000	0.0925
minor groove	0.0000	0.0035	0.0050	0.0095
phosphate and major groove	0.0225	0.0290	0.0525	0.0420
phosphate and minor groove	0.0350	0.0315	0.0425	0.0470

Additional Simulations

Additional simulations were performed to investigate direct binding of Mg^{2+} ions at the phosphate backbone and major groove of dsDNA. At the phosphate backbone, all 20 divalent ions were initially placed within 3 Å of the phosphate oxygen atoms. After energy minimization and throughout equilibration simulations, 18 divalent ions remained directly bound to the phosphate backbone for all ions studied. The Mg^{2+} simulation was extended for 200 ns, during which 18 Mg^{2+} ions remained directly bound to the phosphate backbone. Within the major groove, 10 divalent ions were initially placed within 3 Å of a guanine N7 or O6 atom. After energy minimization, only 6 Mg^{2+} ions were directly bound to guanine in the major groove. This number reduced to 5 ions after equilibration simulations and 2 ions after 70-ns production simulations. Within the major groove, the majority of these ions form long-lived (> 1 ns) direct contacts that eventually dissociate to form fully hydrated ions.

Results and Discussion

Validation of Divalent Metal Ion Force Field

Bai et al.[4] used buffer equilibration and atomic emission spectroscopy (BE-AES) to count the number of excess divalent ions bound to a 24-mer DNA duplex (5'-GGTGACGAGTGAGCTACTGGGCGG-3') in the presence of 10 mM Na^+ and 2 mM Mg^{2+} or 20 mM Na^+. Pabit et al.[5] used anomalous small-angle X-ray scattering (ASAXS) to count the

number of excess Sr^{2+} ions bound to a 25-mer DNA duplex (5'-GCATCTGGGCTATAAAAGGGCGTCG-3') in the presence of 1 mM Na^{+}.

For comparison to experiment, the excess number of divalent ions bound to dsDNA predicted by simulation was calculated using a similar procedure described by Yoo and Aksimentiev.[6] The total number of divalent ions is counted within cylindrical shells surrounding the DNA duplex. The concentration of divalent ions in each cylindrical shell is then compared to bulk concentration for a cylindrical shell of the same volume. The excess number of divalent ions within each shell relative to bulk concentration is summed over all space. This summation increases as the cylindrical shell radius increases and converges to a constant number at large distances from the DNA duplex. The converged number is reported as the number of excess ions associated with dsDNA relative to bulk ion concentration. For convenience in this work, the concentration of divalent ions near DNA is calculated using the total number of divalent ions bound to DNA (obtained using methods described in Computational Methods) and the volume of a cylinder defined by the height of the DNA duplex and a radius defined as $r_{\mathrm{cylinder}} = r_{\mathrm{phosphate}} + r_{\mathrm{indirect}}$, where $r_{\mathrm{phosphate}}$ is the average distance between the DNA duplex axis and the oxygen atoms of the phosphate backbone (9 Å) and r_{indirect} includes the second solvation shell of the divalent ion (5 Å for Mg^{2+} and 6 Å for Ca^{2+}, Sr^{2+}, and Ba^{2+}). This cylinder encompasses the DNA duplex and all divalent ions bound in all DNA binding sites through both direct and indirect binding motifs. Cylindrical shells are then defined surrounding this cylinder with radii increasing by 5 Å. The number of excess ions converges near 70 Å from the DNA duplex axis with fluctuations less than 0.2 ions.

The excess number of divalent ions associated with dsDNA relative to bulk divalent ion concentration is reported in Table S4. The bulk divalent ion concentrations of each simulation are 5 mM, 3 mM, 4 mM, and 5 mM for the Mg^{2+}, Ca^{2+}, Sr^{2+}, and Ba^{2+} simulations, respectively. The number of excess Sr^{2+} ions bound to a slightly longer DNA duplex measured experimentally using ASAXS[5] agrees with simulation within error. In BE-AES experiments, Ca^{2+}, Sr^{2+}, and Ba^{2+} exhibit a size-dependent trend where the number of excess divalent ions decreases with increasing solvated ion radius.[4] The simulations reported in this work predict the same trend and quantitatively reproduce experimental values within error. However, simulation underestimates the number of excess Mg^{2+} ions associated with dsDNA relative to experiment by ~3 ions. This discrepancy may be due to a lack of direct binding between Mg^{2+} and dsDNA predicted by the current force field.

Table S4 Excess number of divalent ions associated with dsDNA.

ion	BE-AES experiment[a]		ASAXS experiment[b]	Simulation[c]
	10 mM Na^+, 2 mM Mg^{2+}	20 mM Na^+	1 mM Na^+	10 mM Na^+
Mg^{2+}	n/a	18	n/a	15 ± 1
Ca^{2+}	15	18	n/a	17 ± 1
Sr^{2+}	14	19	19 ± 2	16 ± 1
Ba^{2+}	13	17	n/a	15 ± 1

a Bai et al.[4] Bulk divalent ion concentration is 6 mM (10 mM Na^+, 2 mM Mg^{2+}) or 5 mM (20 mM Na^+). Typical experimental error is $\pm$ 2 ions.

b Pabit et al.[5] Bulk divalent ion concentration is not reported. Total divalent ion concentration is 10 mM.

c This work. Bulk divalent ion concentration is ~5 mM. Error reported as standard deviation of time-averaged ion count.

Divalent metal ions are expected to displace monovalent ions near the surface of dsDNA due to the stronger Coulombic potential of divalent ions compared to monovalent ions.[4,6–9] The occupancy of dsDNA by monovalent (Na^+) and divalent (Ni^{2+}, Co^{2+}, Mg^{2+}, Ca^{2+}, Sr^{2+}, or Ba^{2+}) ions is shown in Fig. S3. Bound ions are defined by a distance cutoff of 5 Å (Na^+, Ni^{2+}, Co^{2+}, Mg^{2+}) or 6 Å (Ca^{2+}, Sr^{2+}, Ba^{2+}) from any DNA atom, which accounts for both direct and indirect binding between the metal ions and dsDNA. For all divalent ions studied here, the occupancy of the divalent ion is much larger than the monovalent ion. Therefore, divalent ions displace monovalent ions near the DNA surface.

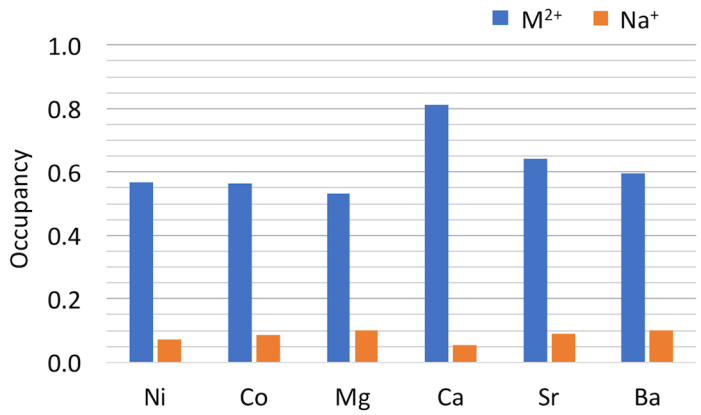

Fig. S3 Occupancy of dsDNA by monovalent (Na^+) and divalent (M^{2+}, M = Ni, Co, Mg, Ca, Sr, or Ba) metal ions.

Force field parameters of divalent metal ions may overestimate their interaction with phosphate and carboxylate groups.[2,10–16] Experimentally measured ion-phosphate distances are available for Mg^{2+}, Ni^{2+}, and Co^{2+} ions directly bound to phosphate groups.[17,18] Although direct binding of these ions to dsDNA is not observed when all divalent ions are initially placed far from the phosphate backbone (> 8 Å), additional simulations were performed with all divalent ions initially placed within direct binding distance of the phosphate backbone (< 3 Å). Ion-phosphate distances from these simulation are compared to experimental and computational values in Table S5. The force field parameters developed by Li et al.[1] underestimate the Mg^{2+}–P distance relative to the experimental value, but not as severely as other Mg^{2+} parameters. The parameters optimized by Allner et al.[10] perform slightly better than the parameters used in this work. Experimental distances are not available for Mg^{2+} ions indirectly bound to the phosphate

backbone, but a previous simulation using the Allner et al. parameters report a Mg^{2+}–O distance of 4.2 Å,[10] which is reproduced by the parameters used in this work (see Fig. 3).

Table S5. Ion-Phosphate Distances of Divalent Metal Ions Directly Bound to Phosphate Groups

ion-phosphate distance	method	distance (Å)
Mg^{2+}–P	Li et al.[a]	3.36
	Allnér et al.[b]	3.41
	LB-Aqvist[b]	3.35
	CHARMM[b]	3.30
	experiment[c]	3.6
Ni^{2+}–O	Li et al.[a]	1.78
	experiment[d]	2.05
Co^{2+}–O	Li et al.[a]	1.84
	experiment[d]	2.09

a This work using divalent force field parameters of Li et al.[1]

b Allnér et al.[10]

c Caminiti et al.[17]

d Inada et al.[18]

For Ni^{2+} and Co^{2+} ions directly bound to phosphate groups, the force field parameters used in this work significantly underestimate Ni^{2+}–O and Co^{2+}–O distances (Table S5). Similar underestimation of ion-oxygen distances between these transition metal ions and water molecules has been improved by using alternative force field models.[16,19] Thus, the Ni^{2+} and Co^{2+} parameters developed by Li et al.[1] to reproduce ion hydration data are not successfully validated for modeling DNA-ion binding for transition metal ions.

DNA Binding Sites

Phosphate Backbone. Divalent metal ions interact with the phosphate backbone of dsDNA through direct binding, indirect binding, and simultaneous direct and indirect binding. The direct and indirect contacts involved in each type of DNA-ion binding can be classified by the relative position(s) of phosphate group(s) involved in the DNA-ion interaction: contacts formed with oxygen atom(s) on the same phosphate residue are labeled "same, " contacts formed with oxygen atoms on phosphate residues next to on another along the same DNA strand are labeled "neighbor," and contacts formed with oxygen atom(s) on phosphate groups separated by at least one residue are labeled "adjacent." Note that adjacent residues may be on the same DNA strand, but are typically on different DNA strands; thus ions bound to adjacent phosphate residues typically span the minor groove of dsDNA.

The number and type of indirect contacts formed between divalent metal ions and the phosphate backbone are shown in Fig. S4. The majority of these ions form one or two hydrogen bonds on the same phosphate group. A small portion form three or more hydrogen bonds that are typically on neighboring phosphate groups. The number and type of contacts for ions that form at least one direct contact with the phosphate backbone are shown in Fig. S5. These ions (Ca^{2+}, Sr^{2+}, and Ba^{2+}) form at most two direct contacts on the same phosphate group. Simultaneous direct and indirect binding typically occurs on the same or neighboring phosphate residue as the direct contact(s). Therefore, all divalent metal ions bound to the phosphate backbone prefer to bind to the same or neighboring phosphate residue(s), regardless of the binding motif (i.e., direct or indirect binding).

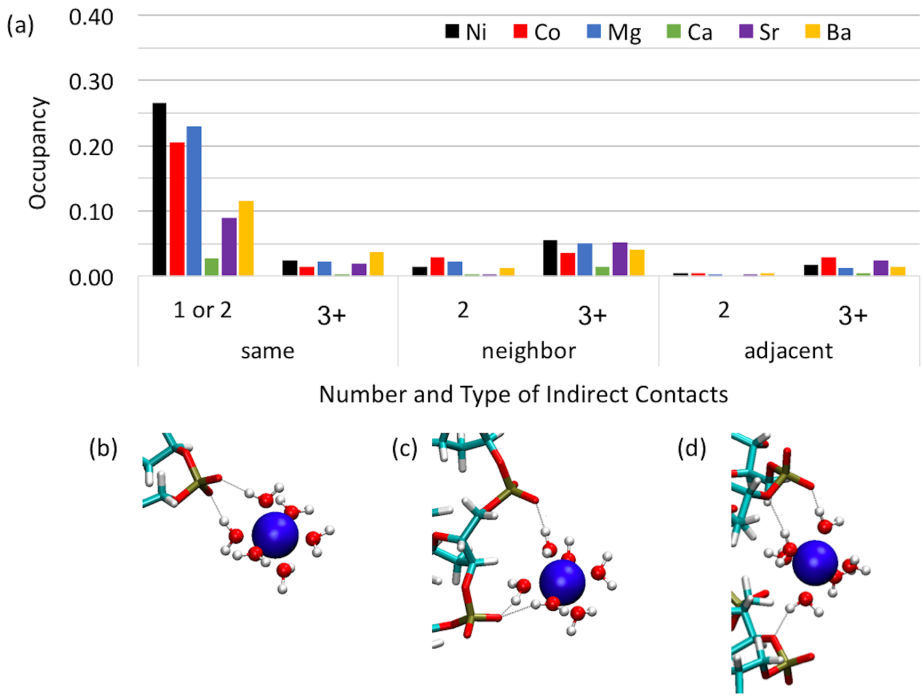

Fig. S4 (a) Occupancy of the phosphate backbone by divalent metal ions through indirect contacts only that are classified as contacts on the same phosphate group (same), phosphate groups next to one another along the same DNA strand (neighbor), and phosphate groups separated by one or more residues, typically on different DNA strands (adjacent). Mg^{2+} and its first solvation shell are shown binding to (b) the same phosphate group, (c) neighboring phosphate groups, and (d) adjacent phosphate groups.

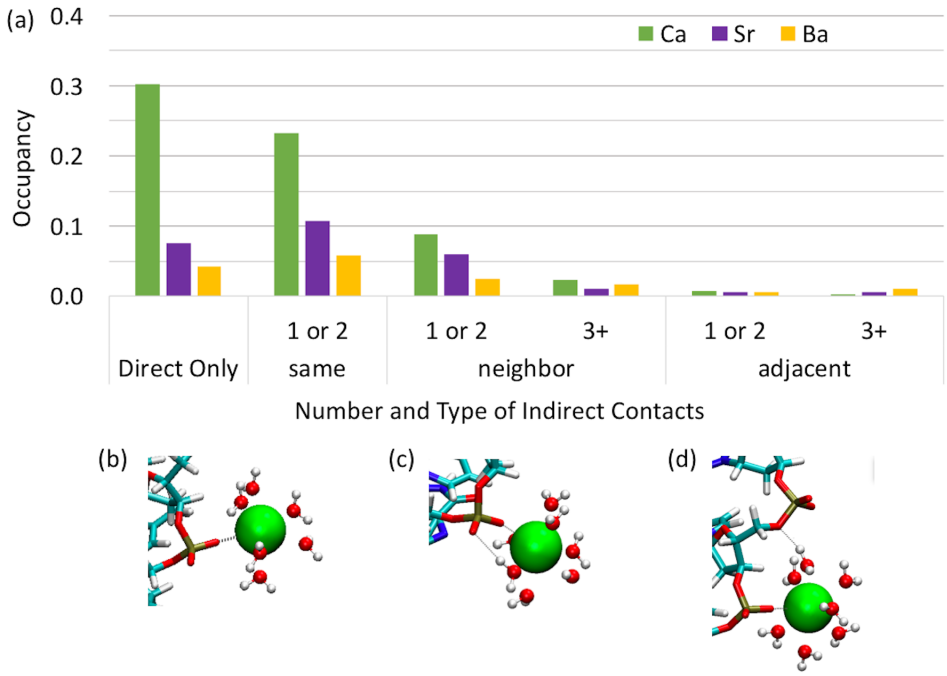

Fig. S5 (a) Occupancy of the phosphate backbone by divalent metal ions through direct contacts only (Direct Only) or simultaneous direct and indirect contacts, which are classified as indirect contacts on the same phosphate group as the direct contact(s) (same), indirect contacts on phosphate group(s) next to the phosphate group with the direct contact(s) (neighbor), and indirect contacts on phosphate group(s) separated by one or more residues from the phosphate group with the direct contact(s) (adjacent). Ca^{2+} and its first solvation shell are shown with (b) one direct contact, (c) one direct contact and one indirect contact on the same phosphate group, and (d) one direct contact and one indirect contact on neighboring phosphate groups.

Minor Groove. The RDFs for each divalent metal ion and the electronegative atoms in the minor groove (N3 of adenine, O2 of thymine, N3 of guanine, and O2 of cytosine) are shown in Fig. S6. The only notable peak is a small peak in the Co^{2+} RDF for thymine O2 (Fig. S6b), which is located in the second solvation shell of Co^{2+}. There is a small probability that Co^{2+} indirectly binds to the O2 atom of thymine in the minor groove, which is consistent with a small occupancy of the minor groove for Co^{2+} (Table S6).

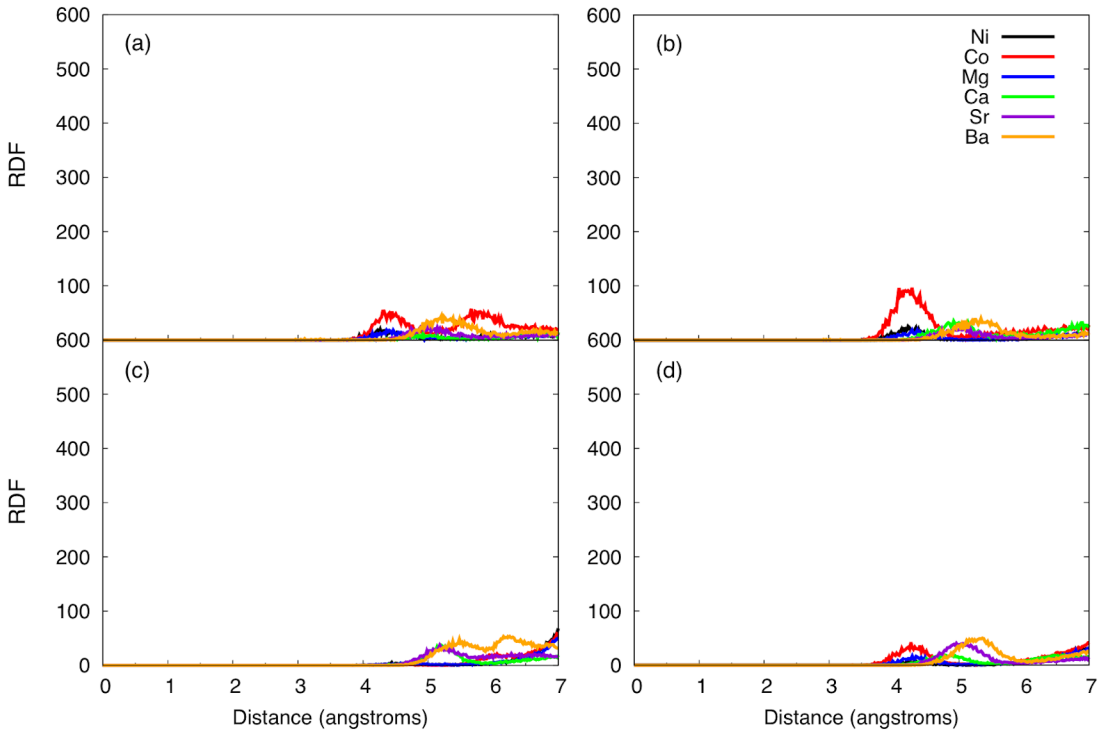

Fig. S6 The RDFs between each divalent metal ion and the (a) N3 atom of adenine, (b) O2 atom of thymine, (c) N3 atom of guanine, and (d) O2 atom of cytosine in the minor groove.

Major Groove. The RDFs for each divalent metal ion and the electronegative atoms in the major groove (N7 of adenine, O4 of thymine, N7 of guanine, and O6 of guanine) are shown in Fig. S7. The RDF peaks for guanine N7 and O6 atoms are significantly larger than that of adenine N7 and thymine O4; therefore, guanine N7 and O6 are the preferred binding sites within the major groove of dsDNA.

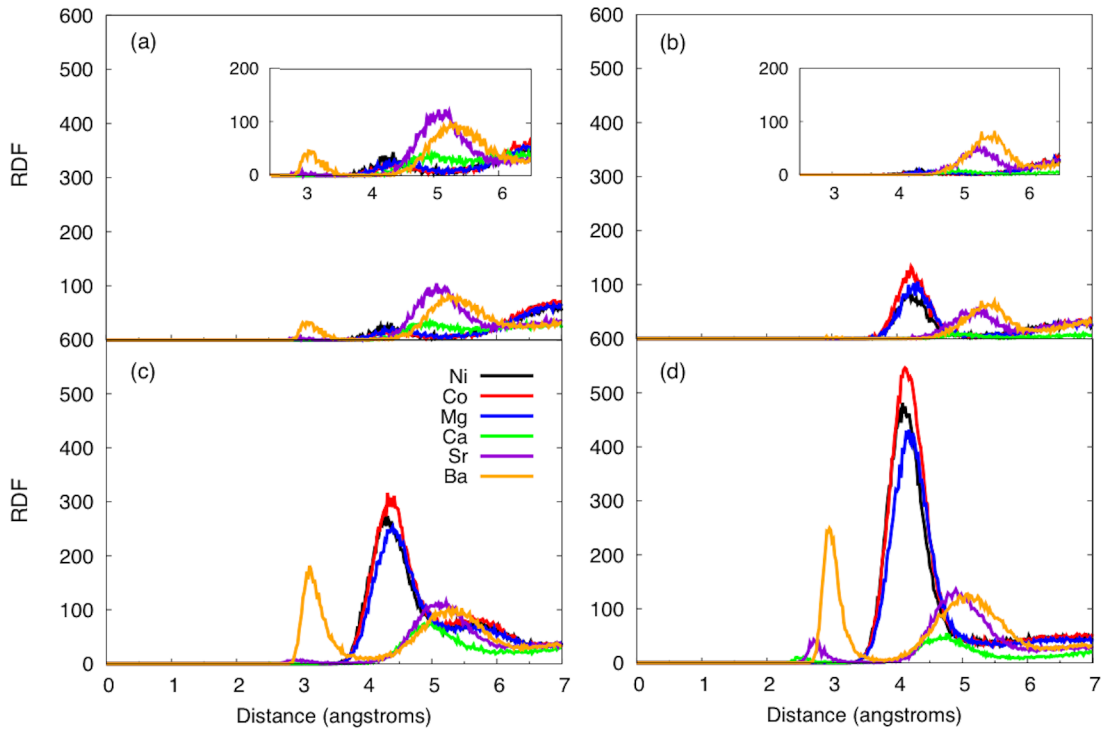

Fig. S7 The RDFs between each divalent metal ion and the (a) N7 atom of adenine, (b) O4 atom of thymine, (c) N7 atom of guanine, and (d) O6 atom of guanine in the major groove of dsDNA. Insets in panels (a) and (b) exclude AT base pairs next to GC base pairs.

Although the RDF peaks of adenine N7 and thymine O4 are small relative to the N7 and O6 atoms of guanine, divalent metal ions may still bind to these atoms. The DNA duplex sequence studied here (Fig. 1a) has an adenine-thymine (AT) track sandwiched by guanine-cytosine (GC) base pairs. Binding to an AT base pair may be due to simultaneous contacts with a neighboring GC base pair. To test this hypothesis the RDFs of adenine N7 and thymine O4 were recalculated without AT base pairs next to GC base pairs in the DNA sequence; these RDFs are shown as insets in panels (a) and (b) of Fig. S7. The RDF peaks of Ni^{2+}, Co^{2+}, Mg^{2+} at the O4 atom of thymine are significantly reduced when AT base pairs neighboring GC base pairs are removed (Fig. S7b and inset). Therefore, the small portion of Ni^{2+}, Co^{2+}, Mg^{2+} ions bound to thymine O4 is likely due to the presence of a nearby N7 or O6 atom of guanine rather than the O4 atom of thymine.

The Ca^{2+}, Sr^{2+}, and Ba^{2+} RDFs calculated for adenine N7 and thymine O4 excluding those next to a GC base pair are similar to those calculated for all AT base pairs (Figs. S7a and S7b, respectively). Therefore, binding of Ca^{2+}, Sr^{2+}, and Ba^{2+} ions to adenine N7 and thymine O4 is independent of neighboring GC base pairs. One explanation may be that the small portion of Ca^{2+}, Sr^{2+}, and Ba^{2+} ions bound to adenine N7 and thymine O4 are simultaneously bound to the phosphate backbone, where the large ionic radius of these ions allows for the water molecules in their first solvation shells to form hydrogen bonds with both the major groove and the phosphate backbone. Overall, divalent metal ions bound to AT base pairs are likely present due to interactions with neighboring GC base pairs or simultaneous binding to the phosphate backbone.

Within the major groove, direct and indirect contacts can be classified by the relative position(s) of the nucleotide(s) involved in the DNA-ion interaction: contacts formed with the same nucleotide are labeled "same," contacts formed with nucleotides next to one another along the same DNA strand are labeled "neighbor," contacts formed between neighboring nucleotides and their respective base pairs are labeled "basepair," and contacts formed with nucleotides separated by at least one residue are labeled "adjacent." Note that basepair contacts necessarily involve both strands of the DNA duplex, whereas adjacent contacts may involve only one DNA strand, but typically involve both strands.

The number and type of indirect contacts formed between divalent metal ions and the electronegative atoms of the major groove are shown in Fig. S8. Within the major groove, divalent metal ions typically form three or more hydrogen bonds to neighboring or basepair residues. Although a larger portion of metal ions bind to the phosphate backbone compared to the major

groove (see Fig. 5), metal ions bound to the major groove form more hydrogen bonds than those bound to the phosphate backbone.

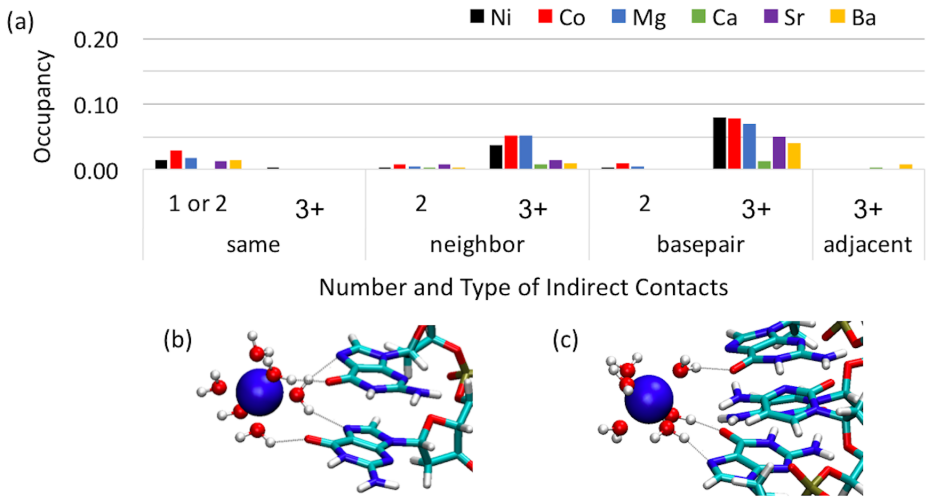

Fig. S8 (a) Occupancy of the major groove by divalent metal ions through indirect contacts only. Bound ions are classified by the number and type of simultaneous indirect contacts. The type of indirect contact(s) is classified as contacts on the same residue (same), contacts on residues next to one another within the same DNA strand (neighbor), contacts on base pair residues and their neighbor residues (basepair), and contacts on residues separated by one or more residues (adjacent). Mg^{2+} and its first solvation shell are shown binding to (b) neighbor residues and (c) basepair residues in the major groove.

Ca^{2+} does not form direct contacts with the electronegative atoms within the major groove of dsDNA, but a small portion of Sr^{2+} and Ba^{2+} ions form simultaneous direct and indirect contacts within the major groove (Fig. 7b). Sr^{2+} forms up to one direct contact, whereas Ba^{2+} forms up to two direct contacts on the same, neighboring, or basepair residues. For both Sr^{2+} and Ba^{2+}, direct binding is typically accompanied by up to three indirect contacts on neighboring or basepair residues relative to the direct contact(s).

Quantitative Analysis of DNA-Ion Binding

Occupancy values shown in Fig. 5 are provided in Table S6. The Ni^{2+} and Co^{2+} occupancy values are also provided in Table S6. Error is reported as the standard deviation of time averages.

Table S6. Occupancy of DNA binding sites by divalent metal ions.[a]

binding site	Ni^{2+}	Co^{2+}	Mg^{2+}	Ca^{2+}	Sr^{2+}	Ba^{2+}
total occupancy	0.5350 ± 0.0041	0.5325 ± 0.0040	0.5000 ± 0.0047	0.7925 ± 0.0026	0.6075 ± 0.0044	0.5825 ± 0.0044
phosphate backbone	0.3825 ± 0.0048	0.3200 ± 0.0050	0.3400 ± 0.0043	0.7075 ± 0.0037	0.4550 ± 0.0053	0.3825 ± 0.0058
major groove	0.1400 ± 0.0029	0.1775 ± 0.0019	0.1500 ± 0.0020	0.0250 ± 0.0013	0.0950 ± 0.0026	0.1000 ± 0.0027
minor groove	0.0075 ± 0.0009	0.0300 ± 0.0015	0.0075 ± 0.0009	0.0050 ± 0.0008	0.0000	0.0050 ± 0.0008
phosphate and major groove	0.0050 ± 0.0008	0.0025 ± 0.0006	0.0025 ± 0.0006	0.0425 ± 0.0026	0.0225 ± 0.0017	0.0525 ± 0.0017
phosphate and minor groove	0.0000	0.0025 ± 0.0006	0.0000	0.0125 ± 0.0018	0.0350 ± 0.0022	0.0425 ± 0.0022

a Number of bound ions calculated using python script (see Computational Methods). Error is standard deviation of time averages.

Sequence-Dependent Binding in Major Groove

The occupancy of each base pair at the phosphate backbone and the major groove of dsDNA is shown in Fig. S9. Base pairs are labeled by the nucleotide sequence (5'-GGCGGCGGCGCGGCGTTTTTTGG-3'), where the terminal two base pairs on either end of the DNA duplex are omitted from analysis. For all divalent ions studied, occupancy at the phosphate backbone is distributed along the DNA duplex, whereas occupancy in the major groove is larger

for GC base pairs compared to AT base pairs. Some binding at AT base pairs is observed, which is likely due to simultaneous binding to a neighboring guanine residue or the phosphate backbone (see Fig. S7). This sequence-dependent binding within the major groove is consistent with second harmonic generation studies of single-strand DNA, where cytosine and guanine oligonucleotides bind more Mg^{2+} ions per strand compared to adenine and thymine oligonucleotides.[20] Ion counting experiments with dsDNA report sequence-independent results for Mg^{2+}, Ca^{2+}, Sr^{2+}, and Ba^{2+},[4] which is consistent with sequence-independent binding at the phosphate backbone predicted by simulation.

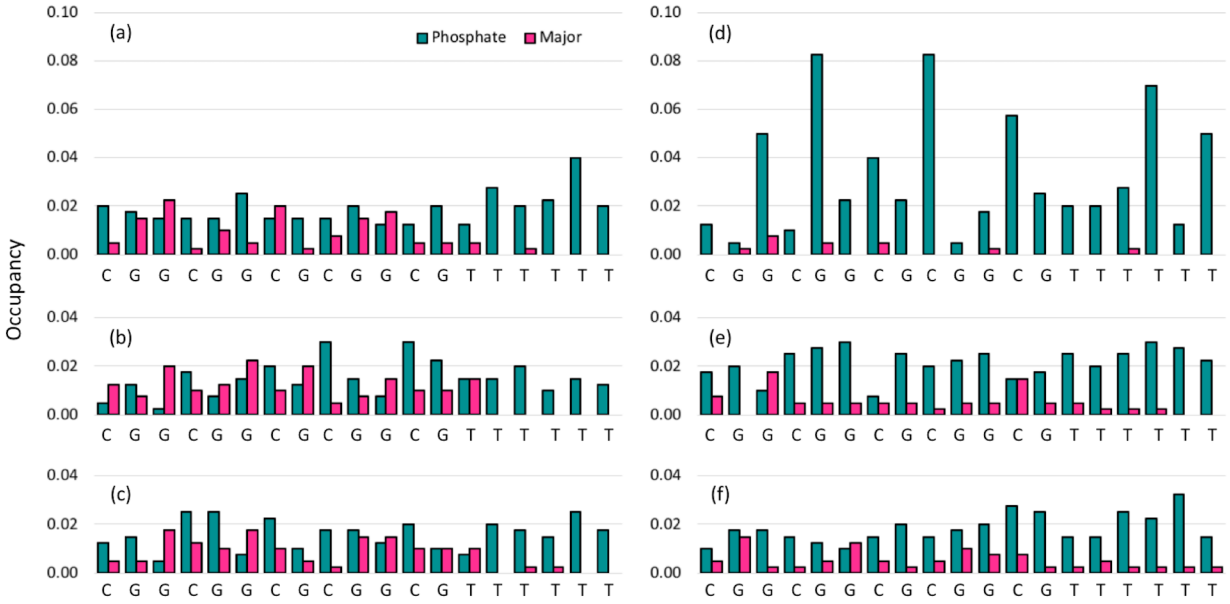

Fig. S9 Occupancy of DNA base pairs at the phosphate backbone (Phosphate) and major groove (Major) for (a) Ni^{2+}, (b) Co^{2+}, (c) Mg^{2+}, (d) Ca^{2+}, (e) Sr^{2+}, and (f) Ba^{2+} ions.

Major Groove Binding at Guanine N7 and O6 Atoms

The occupancy of four electronegative atoms within the major groove of dsDNA due to indirect only or simultaneous direct and indirect contacts is shown in Fig. S10, where each bound ion is classified by its shortest contact. For indirect binding only, the occupancies of both the N7 and O6 atoms of guanine are significantly larger for metal ions more closely bound to the O6 atom (Fig. S10b) rather than the N7 atom (Fig. S10a). There is significant occupancy of both the N7 and O6 atomic sites, regardless of which atomic site forms the shortest contact with the bound metal ion. Therefore, the majority of divalent metal ions bound to the major groove of dsDNA form simultaneous interactions with both the N7 and O6 atoms of guanine with slightly shorter interactions with O6 compared to N7. Similar results are observed for simultaneous direct and indirect binding of Sr^{2+} and Ba^{2+} within the major groove.

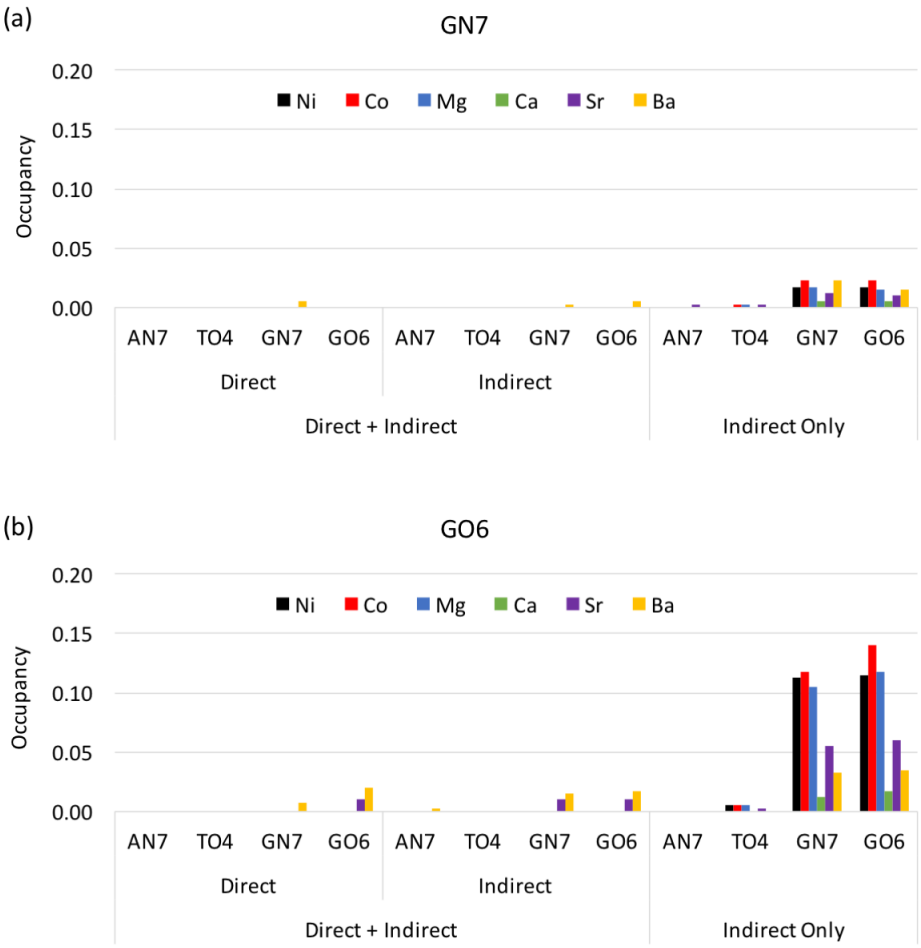

Fig. S10 Occupancy of electronegative atoms within the major groove of dsDNA, where the shortest contact of each metal ion is formed with the (a) N7 atom of guanine or the (b) O6 atom of guanine. Bound ions are classified by the type of contact(s): simultaneous direct and indirect contacts (Direct + Indirect), or indirect contact(s) only (Indirect Only).

Overall Comparison of Alkaline Earth Metal Ions

Occupancy of the phosphate backbone or major groove by alkaline earth metal ions Ca^{2+}, Sr^{2+} and Ba^{2+} with a given number of water molecules in their first solvation shells is shown in Fig. S11. Compared to the coordination numbers of each metal ion simulated in aqueous solution

without dsDNA reported by Li et al.,[1] direct binding is typically accompanied by the loss of at least one water molecule from the first solvation shell of each ion.

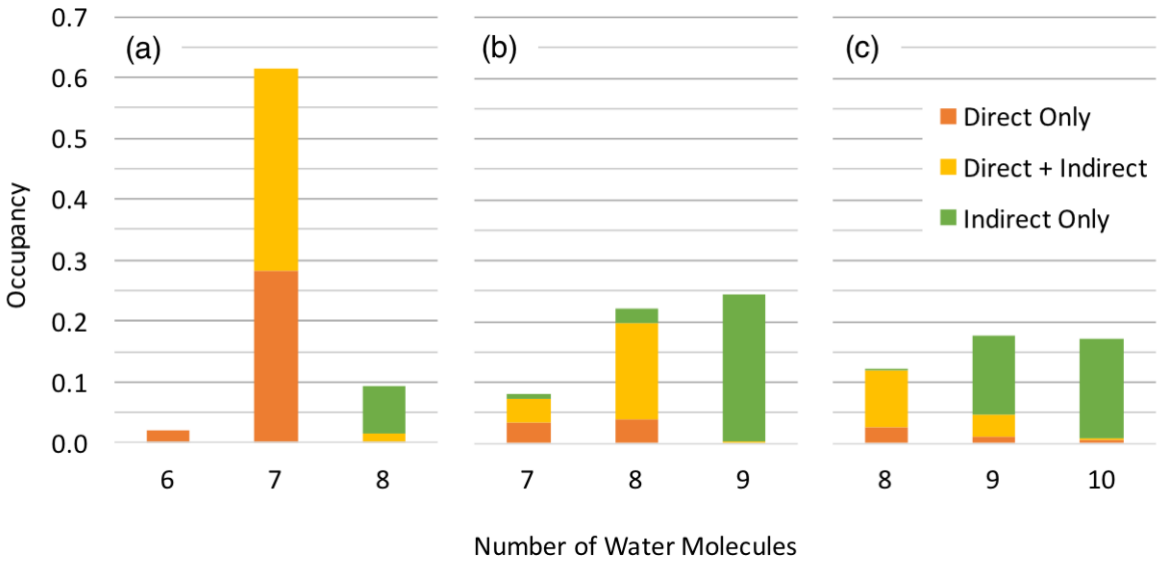

Fig. S11 Occupancy of the phosphate backbone or the major grove of dsDNA by (a) Ca^{2+}, (b) Sr^{2+} and (c) Ba^{2+} ions with a given number of water molecules in their first solvation shells. Bound ions are classified by the type of contact(s): direct contact(s) only (Direct Only), simultaneous direct and indirect contacts (Direct + Indirect), or indirect contact(s) only (Indirect Only).

The average number of binding events per ion and the distribution of residence times are shown in Figs. S12 and S13, respectively. The error bars report the standard deviation of 20 divalent metal ions present in each simulation; therefore, a large error bar indicates a large variation among divalent ions within the same simulation. Ni^{2+}, Co^{2+}, Mg^{2+}, and Ca^{2+} have a similar number of binding events per ion and that number increases with increasing ionic radius for Sr^{2+} and Ba^{2+}. The average number of binding events per Ca^{2+} ion is small at the phosphate backbone, because these ions are likely to form direct contacts with the oxygen atoms of the phosphate

backbone with long residence times (> 1 ns). In contrast, Sr^{2+} and Ba^{2+} ions have more binding events with shorter residence times. As the ionic radius increases ($Ca^{2+} < Sr^{2+} < Ba^{2+}$), the number of direct binding events at the phosphate backbone increases and the average residence time of each direct contact decreases. Ni^{2+}, Co^{2+}, and Mg^{2+} ions interact with DNA through indirect contacts only and have more intermediate residence times (500 ps – 1 ns) at the phosphate backbone compared to the larger ions with variable first solvation shells (Ca^{2+}, Sr^{2+}, and Ba^{2+}). Within the major groove, Ca^{2+}, Sr^{2+}, and Ba^{2+} form many short-lived (< 500 ps) contacts. Although the average number of binding events for Ni^{2+}, Co^{2+}, and Mg^{2+} in the major groove is small relative to Ca^{2+}, Sr^{2+}, and Ba^{2+}, these ions have long-lived (> 1 ns) residence times.

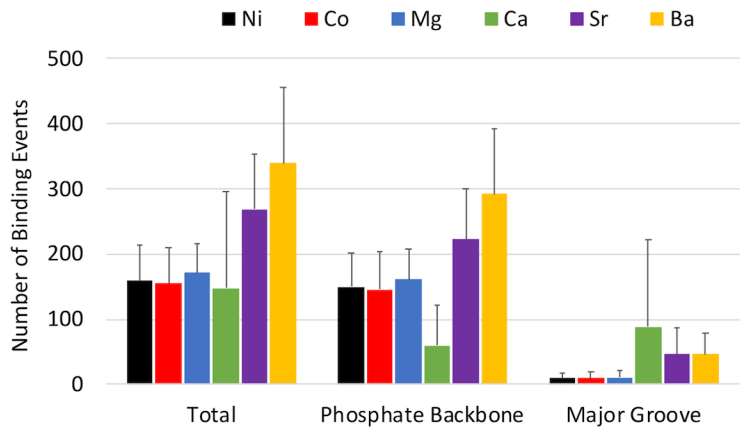

Fig. S12 Average number of binding events per ion at the phosphate backbone or major groove (Total), phosphate backbone only (Phosphate Backbone), and major groove only (Major Groove). Error is the standard deviation of 20 divalent metal ions in each simulation.

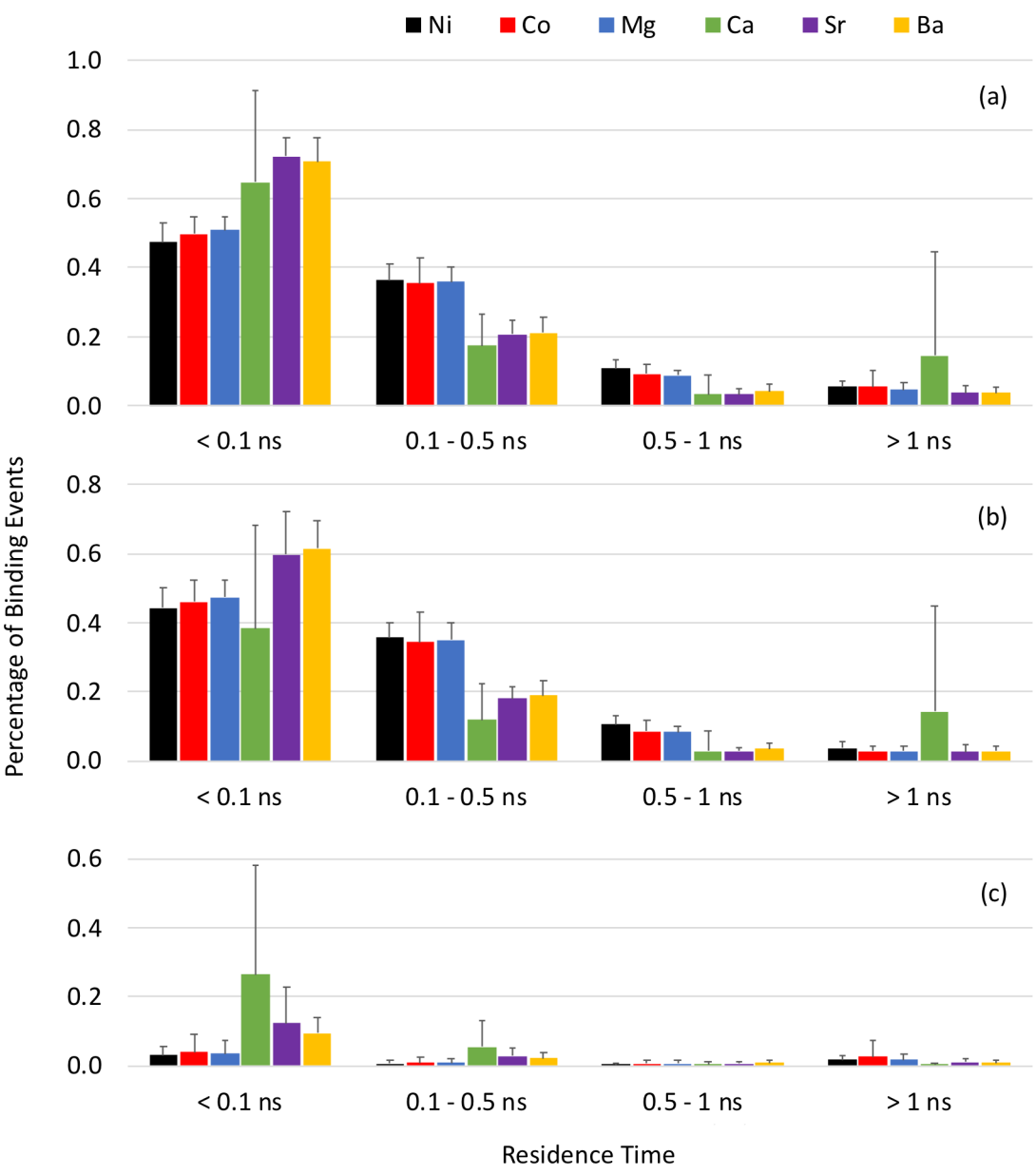

Fig. S13 Distribution of residence times for binding events at the (a) phosphate backbone or major groove, (b) phosphate backbone only, and (c) major groove only. Values are reported as an average percentage of binding events for each ion. Error is the standard deviation of 20 divalent metal ions in each simulation.

References

1 P. Li, B. P. Roberts, D. K. Chakravorty and K. M. Merz, Rational Design of Particle Mesh Ewald Compatible Lennard-Jones Parameters for +2 Metal Cations in Explicit Solvent., *J. Chem. Theory Comput.*, 2013, **9**, 2733–2748.

2 J. Yoo, J. Wilson and A. Aksimentiev, Improved model of hydrated calcium ion for molecular dynamics simulations using classical biomolecular force fields, *Biopolymers*, 2016, **105**, 752–763.

3 J. Wen, X. Shen, H. Shen and F.-S. Zhang, Hofmeister series and ionic effects of alkali metal ions on DNA conformation transition in normal and less polarised water solvent, *Mol. Phys.*, 2014, **112**, 2707–2719.

4 Y. Bai, M. Greenfeld, K. J. Travers, V. B. Chu, J. Lipfert, S. Doniach and D. Herschlag, Quantitative and Comprehensive Decomposition of the Ion Atmosphere around Nucleic Acids, *J. Am. Chem. Soc.*, 2007, **129**, 14981–14988.

5 S. A. Pabit, S. P. Meisburger, L. Li, J. M. Blose, C. D. Jones and L. Pollack, Counting Ions around DNA with Anomalous Small-Angle X-ray Scattering, *J. Am. Chem. Soc.*, 2010, **132**, 16334–16336.

6 J. Yoo and A. Aksimentiev, Competitive binding of cations to duplex DNA revealed through molecular dynamics simulations., *J. Phys. Chem. B*, 2012, **116**, 12946–12954.

7 W. Li, L. Nordenskiöld and Y. Mu, Sequence-specific Mg^{2+}-DNA interactions: a molecular dynamics simulation study., *J. Phys. Chem. B*, 2011, **115**, 14713–14720.

8 R. Das, T. T. Mills, L. W. Kwok, G. S. Maskel, I. S. Millett, S. Doniach, K. D. Finkelstein, D. Herschlag and L. Pollack, Counterion Distribution around DNA Probed by Solution X-Ray Scattering, *Phys. Rev. Lett.*, 2003, **90**, 188103.

9 K. Andresen, R. Das, H. Y. Park, H. Smith, L. W. Kwok, J. S. Lamb, E. J. Kirkland, D. Herschlag, K. D. Finkelstein and L. Pollack, Spatial Distribution of Competing Ions around DNA in Solution, *Phys. Rev. Lett.*, 2004, **93**, 248103.

10 O. Allnér, L. Nilsson and A. Villa, Magnesium Ion–Water Coordination and Exchange in Biomolecular Simulations, *J. Chem. Theory Comput.*, 2012, **8**, 1493–1502.

11 J. Yoo and A. Aksimentiev, Improved Parametrization of Li^+, Na^+, K^+, and Mg^{2+} Ions for All-Atom Molecular Dynamics Simulations of Nucleic Acid Systems, *J. Phys. Chem. Lett.*, 2012, **3**, 45–50.

12 F. Duarte, P. Bauer, A. Barrozo, B. A. Amrein, M. Purg, J. Aqvist and S. C. L. Kamerlin, Force field independent metal parameters using a nonbonded dummy model., *J. Phys. Chem. B*, 2014, **118**, 4351–4362.

13 P. Satpati, C. Clavaguéra, G. Ohanessian and T. Simonson, Free Energy Simulations of a GTPase: GTP and GDP Binding to Archaeal Initiation Factor 2, *J. Phys. Chem. B*, 2011,

115, 6749–6763.

14 T. Simonson and P. Satpati, Simulating GTP:Mg and GDP:Mg with a simple force field: A structural and thermodynamic analysis, *J. Comput. Chem.*, 2013, **34**, 836–846.

15 J. Melcr, H. Martinez-Seara, R. Nencini, J. Kolafa, P. Jungwirth and O. H. S. Ollila, Accurate Binding of Sodium and Calcium to a POPC Bilayer by Effective Inclusion of Electronic Polarization, *J. Phys. Chem. B*, 2018, **122**, 4546–4557.

16 G. Chillemi, P. D'Angelo, N. V. Pavel, N. Sanna and V. Barone, Development and Validation of an Integrated Computational Approach for the Study of Ionic Species in Solution by Means of Effective Two-Body Potentials. The Case of Zn^{2+}, Ni^{2+}, and Co^{2+} in Aqueous Solutions, *J. Am. Chem. Soc.*, 2002, **124**, 1968–1976.

17 R. Caminiti, Complex formation and phosphate-H_2O interactions in a concentrated aqueous $Mg(H_2PO_4)^2$ solution., *J. Mol. Liq.*, 1984, **28**, 191–204.

18 Y. Inada, H. Hayashi, K. Sugimoto and S. Funahashi, Solvation Structures of Manganese(II), Iron(II), Cobalt(II), Nickel(II), Copper(II), Zinc(II), and Gallium(III) Ions in Methanol, Ethanol, Dimethyl Sulfoxide, and Trimethyl Phosphate As Studied by EXAFS and Electronic Spectroscopies, *J. Phys. Chem. A*, 1999, **103**, 1401–1406.

19 P. Li and K. M. Merz, Taking into Account the Ion-Induced Dipole Interaction in the Nonbonded Model of Ions, *J. Chem. Theory Comput.*, 2014, **10**, 289–297.

20 J. G. Holland, J. N. Malin, D. S. Jordan, E. Morales and F. M. Geiger, Specific and nonspecific metal ion-nucleotide interactions at aqueous/solid interfaces functionalized with adenine, thymine, guanine, and cytosine oligomers., *J. Am. Chem. Soc.*, 2011, **133**, 2567–2570.